

## Gap-plasmon enhanced water splitting with ultrathin hematite films: The role of plasmonic-based light trapping and hot electrons

Aveek Dutta,<sup>a,b</sup> Alberto Naldoni,<sup>\*c</sup> Francesco Malara,<sup>d</sup> Alexander Govorov,<sup>e</sup> Vladimir M. Shalaev<sup>a,b</sup> and Alexandra Boltasseva<sup>\*a,b</sup>

<sup>a</sup> School of Electrical and Computer Engineering, Purdue University, IN-47907, USA.

<sup>b</sup> Birck Nanotechnology Center, Purdue University, West Lafayette, IN-47907, USA.

<sup>c</sup> Regional Center for Advanced Technologies and Materials, Olomouc-78371, Czech Republic.

<sup>d</sup> CNR-Istituto di Scienze e Tecnologie Molecolari, Via Golgi 19, 20133 Milan, Italy

<sup>e</sup> Department of Physics and Astronomy, Ohio University, Athens OH-45701, USA

### SUPPLEMENTARY INFORMATION

#### Methods

*Raman*- The sample was put on a metal plate, and excitation laser was focused on its surface and tuned to maximize the analytic signal. The laser power on the sample was set to 1 mW to minimize damage caused by the radiation. Exposition time was 3s. Each measured Raman spectrum was an average of 1024 experimental microscans. Raman spectra were evaluated using instrument control software (Omnic, version 8, Thermo Scientific, USA) and plotted by QtiPlot (ProIndep Serv S.r.l., Romania).

*TEM*- The thin film from sample was scratched off by blade and dispersed in ethanol, sonicated for 5 minutes and one drop put on copper grid with Holey carbon film. After drying on the air at room temperature were samples measured by HRTEM Titan G2 (FEI) with Image corrector on accelerating voltage 80 kV. Images were taken with BM UltraScan CCD camera (Gatan).

*Ellipsometry and AFM*- The optical constants of the hematite films were obtained through Variable Angle Spectroscopic Ellipsometry (VASE) using a J.A. Woollam V-VASE. The obtained ellipsometry data proved difficult to fit with a known model of Fe<sub>2</sub>O<sub>3</sub>. This is perhaps due to the fact that the bottom gold was not thermally stable at the hematite deposition conditions and suffered from formation of holes. Also the hematite film had a RMS roughness of 2.4nm. This film roughness is 16% of the film thickness. The film roughness was obtained using a Veeco Dimension AFM. So the optical constants shown in Figure S1b gave us the best simulation fit to the reflection spectra of the fabricated Au nanodisks obtained from experiments and donot necessarily reflect the true optical constants of the hematite film. In fact, the reported refractive index of hematite in literature in the visible wavelengths is around 3 which is significantly larger than the “effective” hematite index we use here.

*Fabrication*- After the hematite growth on gold film using PLD, PMMA was spin coated on the hematite at 4000 rpm for 60 secs. Then the sample was soft baked at 180°C for 3 mins. The nanodisk arrays were defined using an e-beam writer. The PMMA was then developed using 1:3 MIBK:IPA solution for 50 secs and rinsed afterwards in IPA for 30 secs. Finally, the gold nanodisks, 50nm height, were deposited on the sample using e-beam evaporation followed by PMMA removal with acetone.

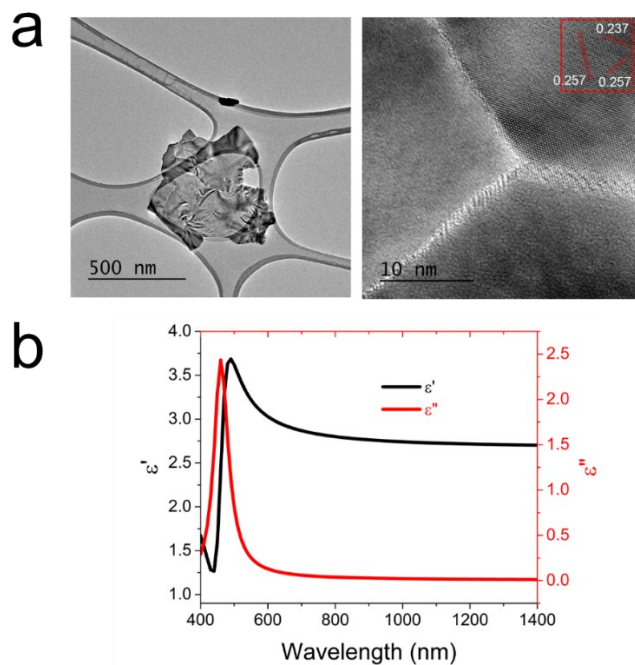


Figure S1: a) (Left) TEM image of the hematite flake scraped from the deposited sample on gold/Si. (Right) HRTEM image of the hematite film repeated from Figure 2b. b) Optical permittivity of the hematite film as extracted from Variable Angle Spectroscopic Ellipsometry.

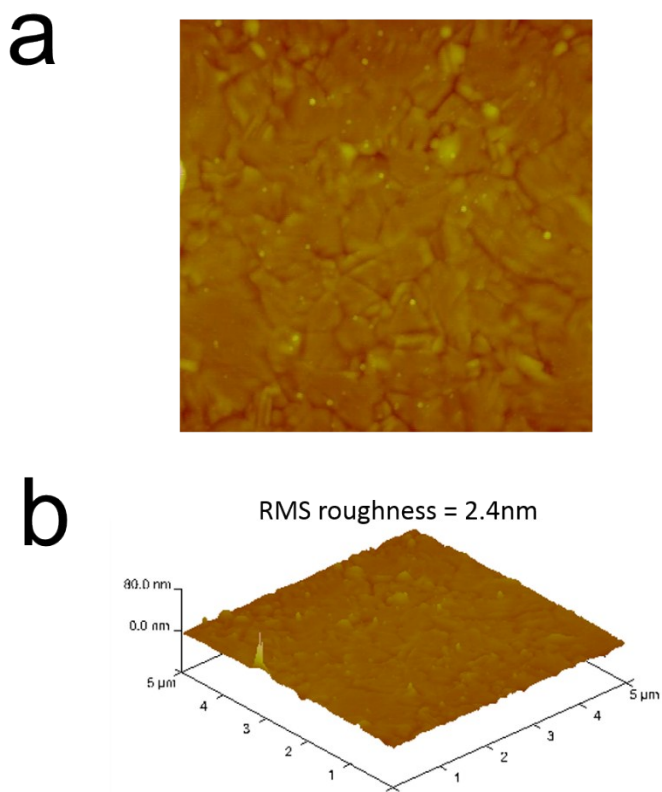


Figure S2: a) AFM scan of a hematite film on gold. b) Section view of the film topology which gives an RMS roughness of 2.4nm

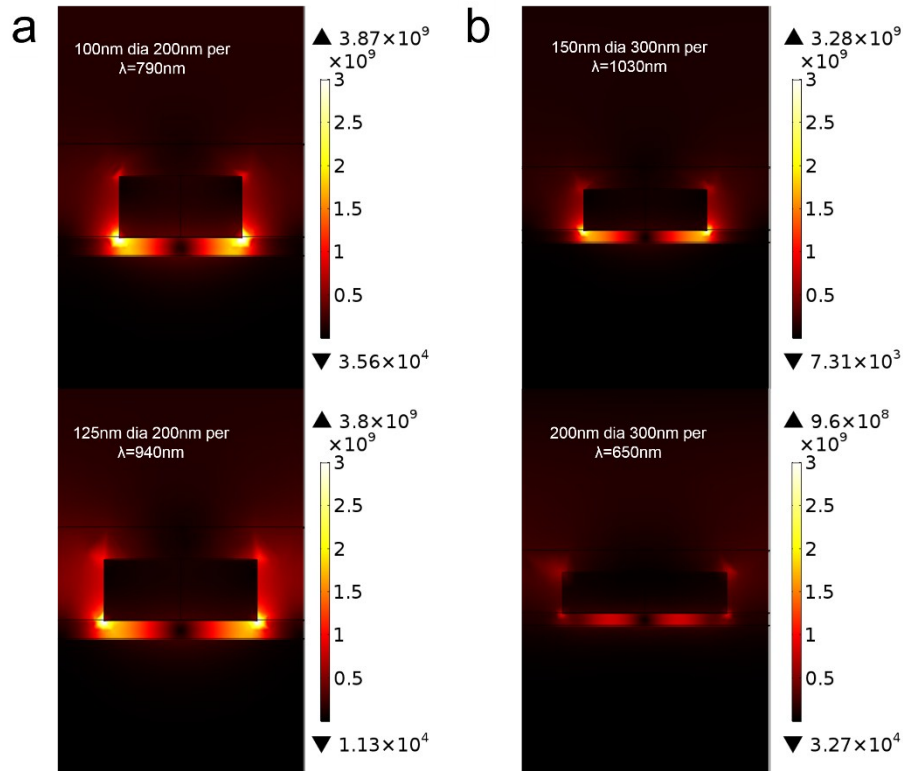


Figure S3: Electric field intensity map for nanodisks with a) 200nm pitch and b) 300nm pitch with two different diameters for each pitch. The field maps are taken at the resonant wavelength corresponding to the absorption peaks in the simulated plots of Figure 3b and 3c. Gap plasmon resonances leading to high field intensity in the hematite layer can be clearly seen. [In the graphs, dia  $\rightarrow$  diameter of nanodisk, per  $\rightarrow$  period of array]

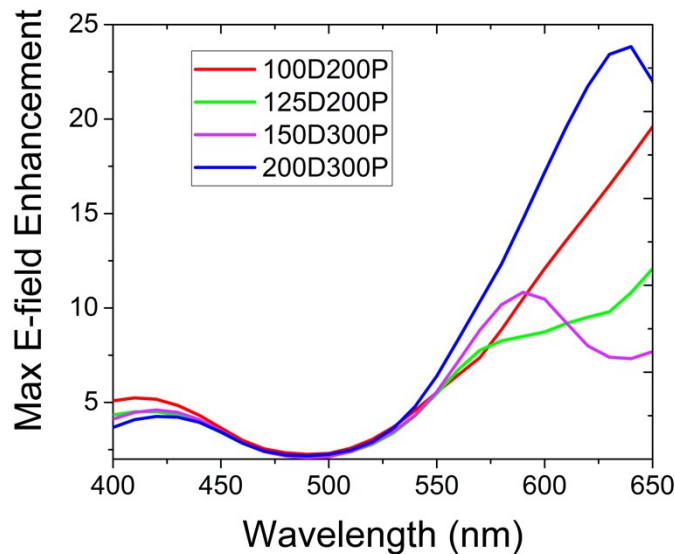


Figure S4: Maximum electric field intensity enhancement as a function of the incident wavelength in the hematite layers for the different arrays compared to a bare film. The simulated enhancement in the above bandgap region is attributed to scattering from the nanodisks and back reflection from the gold mirror. This is believed to lead to the above bandgap photocurrent enhancement observed in experiments. D: diameter of nanodisk and P: Period of array in nanometer.